

A Mini-Review: Quinones and their Derivatives for Selective and Specific Detection of Specific Cations

Bigyan Ranjan Jali¹ 

¹ Department of Technology, Veer Surendra Sai University of Technology Burla, Sambalpur-768018, Odisha, India; bigyan.Jali7@gmail.com (B.R.J.);

* Correspondence: bigyan.Jali7@gmail.com;

Scopus Author ID 36503969200

Received: 14.10.2020; Revised: 11.12.2020; Accepted: 13.12.2020; Published: 16.12.2020

Abstract: The development of fluorescence and colorimetric sensors has been an active research area in the last few decades due to their wide range of environmental, agricultural, and medicinal chemistry applications. This review provides an overview of quinones' recent contribution and their derivatives to fluorescence and colorimetric sensors. It discusses their sensing properties with promising features.

Keywords: fluorescence; chemosensor; color change; UV-visible; quinone.

© 2020 by the authors. This article is an open-access article distributed under the terms and conditions of the Creative Commons Attribution (CC BY) license (<https://creativecommons.org/licenses/by/4.0/>).

1. Introduction

Metal plays a noteworthy role in biological, environmental, and chemical processes. The development of potent molecular probes for selective and specific sensing of specific metal ions is an active research area in the multidisciplinary field of "Supramolecular Chemistry" [1-25]. It has been found that the most widely used receptor contains a signaling unit-spacer-receptor approach. In this approach, the signaling unit is linked through a covalent bond through a spacer. The signaling unit-spacer-receptor model grows up with a substantial contribution by De Silva and his research group [40]. Therefore, an ideal colorimetric and/or fluorescent molecular probe must meet two basic requirements: firstly, the receptor must have the strongest affinity with the relevant target, i.e., binding-selectivity. Secondly, because of good binding-selectivity, its signal should avoid environmental interference, i.e., signal-selectivity [27]. Therefore, it is of great interest to design and synthesis the molecular probes, which properties are modified in the presence of a specific target analyte is a matter of great practical significance [28-30]. In recent reviews, Kumar *et al.*[36], Jose and coworkers [37] have reported various quinone receptors and their photophysical properties. Pope *et al.* [38] described the synthesis and electronic properties of anthraquinones. On the other hand, Skyes and Mariappan reported some examples of anthraquinone derivatives and their cation recognition properties [39]. However, no review article is available exclusively on systematic studies on quinones and their derivatives as sensors for various cations. This review gives an idea of key features of extensively studied about the quinone and its derivatives used for the specific and selective detection of specific cations.

2. Quinones and their Derivatives as Sensors for Cations

Quinones and their derivatives are very important molecular probes due to their various roles in colorimetric and photochemical properties [31-35]. Various fascinating binding sites, <https://biointerfaceresearch.com/>

quinones, and their derivatives show potent molecular probes for various metal salts in the organic solvent, aqueous media, or in both aqueous-organic media. In this section, we wish to discuss various substituted based quinones and their derivatives and their cation sensing properties.

2.1. Quinone tethered amino derivatives.

It is well-known that amino-substituted quinone derivatives act as potent molecular probes for various metal salts such as Group-IA, IIA, transition metals, and lanthanides due to the presence of -NH groups and many binding units. The presence of specific and selective metal ions, color, and spectral change is due to ICT. It is followed by deprotonation of -NH moieties. Carbonyl oxygen of quinone coordinates with metal ions to affect metal-mediated photo-induced charge transfer (PCT) effects. Due to PCT effect, $n-\pi^*$ transitions become higher in energy than corresponding $\pi-\pi^*$ transitions. They switch-ON the fluorescence [40-47]. In these contexts, Kumar and coworkers have reported amino-anthraquinone derivatives **1-4**, which were used for sensing transition metal ions, as shown in figure 1 [44-45]. **1-4** showed noticeable color change upon metal salts' addition (pH 7.0) in CH₃OH-H₂O (1:1, v/v).

Receptor **1** showed absorption maxima at 494 nm in its UV-vis spectrum. The intensity of the absorbance band at 494 nm decreased with a new peak that occurred at 604 nm in the presence of Cu²⁺ ions. It caused the color change from red to blue. It is due to the Cu²⁺ bound selectively with three N-atoms out of two sp² N-atom and one aryl amine N-atom present in the receptor. However, receptor **1** did not induce any color changes and spectral changes upon other metal salts' addition. Receptor **2** displayed the absorption band at 500 nm. The absorption band's intensities at 500 nm decreased, and a new band occurred at 626 nm in the presence of Ni²⁺ and Co²⁺. It caused the color change from red to lilac. However, a new band, the presence of Cu²⁺, occurred at 604 nm with a color change from red to blue.

On the other hand, the receptor remains silent towards other metal ions. It is due to the differential modes of interaction of respective metal ions. Receptor **3** showed the absorbance maxima at 400 nm. The bathochromic shift was perceived due to the presence of Cu²⁺, Ni²⁺, and Co²⁺; it caused the change of color from yellow to brown.

On the other hand, the presence of Zn²⁺ led to a hypsochromic shift and color change from yellow to colorless. It is due to various coordination modes along with multiple optical responses. On continuous effort on the cation sensor, the same group has also reported anthraquinone-based receptors **5-9** based on Schiff base scaffold capable of sensing of various cations in CH₃OH/HEPES (4:1) medium as shown in figure 2 [48-49].

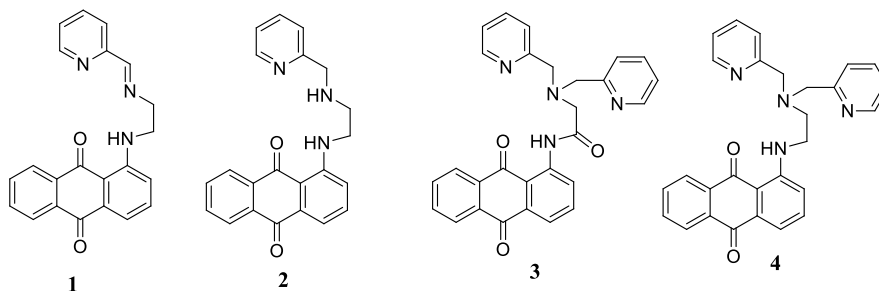


Figure 1. Receptor **1-4** used for sensing properties.

In the UV-vis spectrum, receptor **5** showed the absorbance maxima at 500 nm. The authors found that upon addition of Cu²⁺ and Ni²⁺ to **5**, the color changed from red to blue (Cu²⁺) and green (Ni²⁺). Upon addition of Cu²⁺, a large red shift (100 nm) from absorption maxima

500 to 600 nm takes place but **5**, displayed a mega red shift (250 nm) from absorption maxima 500 to 750 nm in the presence of Ni^{2+} and a new absorption band formed at 385 nm [48]. Due to the existence of amino-anthraquinone moiety and the hydroxyl-naphthalene group, receptor **6** ascribed two absorbance peaks at 500 and 415 nm, respectively. In the presence of Cu^{2+} to **6**, a new absorption peak at 600 nm was observed and associated with the color alteration from red to blue. The authors attributed that the red shift occurred due to the deprotonation of -NH groups. In the presence of Ni^{2+} , the absorbance bands at 500 and 415 nm diminished along with two new absorption bands raised at 445 nm and 700 nm, respectively. The new absorbance band was ascribed due to the deprotonation of both -NH and -OH moiety. The receptor remains silent towards other metal salts. Unlike receptor **6**, receptors **7** showed an absorbance band at 485 nm and 435 nm, respectively, and **8** showed an absorbance band at 492 nm. Both the receptors **7** and **8** found selectively renowned Cu^{2+} . With the addition of Cu^{2+} to **7** and **8**, a large red shift (100 nm) was observed. It caused the color change from red to blue. Receptor **9** showed absorbance maxima at 530 nm. In the presence of Co^{2+} , the absorbance band at 530 nm was quenched, and two new peaks at 365 and 700 nm appeared. It caused the color change to take place from purple to blue. However, in the presence of Ni^{2+} , **9** formed a new broad peak between 700-780 nm, and the purple color goes to blue. The authors suggested that receptor **9** was used for the molecular level information-processing device due to its different optical behaviors [49].

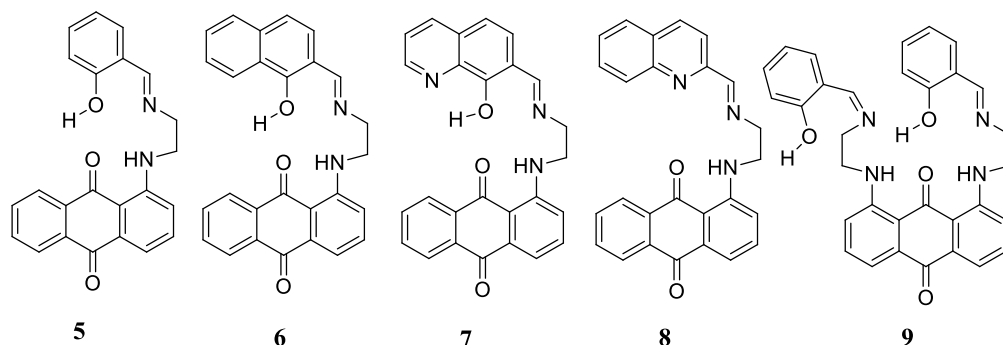


Figure 2. Receptor **5-9** used for sensing properties.

Kaur *et al.* reported the character of Cu^{2+} ions in amino-anthraquinone derivatives **10-12** by using UV-vis spectra ($\text{CH}_3\text{OH-H}_2\text{O}$ 3:1 v/v) at pH 7. Receptor **10** showed absorbance maxima at 512 nm. The absorbance band at 512 nm gradually decrease, and a new peak appeared at 620 nm, and the red color solution turns to blue in the presence of Cu^{2+} . The authors reported that the appearance of a new peak at a higher wavelength due to the formation of **10-Cu²⁺** complex. However, **11** was selectively sensing Cu^{2+} ions amongst other metal salts. The authors suggested that the **10-11-Cu²⁺** complexes were stable up to pH range 4.5-11; at the same time, **11-Cu²⁺** fragmented to give the free receptor and $\text{Cu}(\text{OH})_2$ [48]. In contrast, receptor **12** showed the absorbance band at 492 nm, which was quenched on reacting with of Cu^{2+} (1 equiv.) with a new peak raised at 615 nm. This resulted that the red color solution becomes blue [50]. On continuous effort on their colorimetric chemosensor, the same group also reported anthraquinone-based receptors (**13a-c**); these receptors showed selective towards Cu^{2+} in the presence of other metal salts [52]. The receptors **13a-b** showed absorbance maxima at 492 nm. In the presence of Cu^{2+} ions, new absorption bans have occurred at 600 nm, and the red color solution goes to blue. The authors found that the selectivity Cu^{2+} towards the receptor **13a-b** is due to its highest lewis acid character [53]. The receptors **14a-c** showed absorbance maxima at 535 nm. In the presence of Cu^{2+} , **14a-b**, decreased the absorbance band's intensities

at 535 nm, and two new absorption bands at 715 nm and 800 nm were observed. The magenta color solution turns from purple to blue. It is due to the formation of **14a-b-Cu²⁺** complexes. The receptor **14c** remains silent towards other metal ions, and as well as no color or absorbance change takes place with Cu²⁺ ion [51]. The receptors **15a-c** exhibited an absorption band at 585 nm and 630 nm, respectively. Two new absorption bands raised at around 665 nm in the presence of Cu²⁺ and blue color turn to turquoise blue for **15a-b**. The receptor **15c** remains silent towards other metal salts, as shown in figure 3 [54].

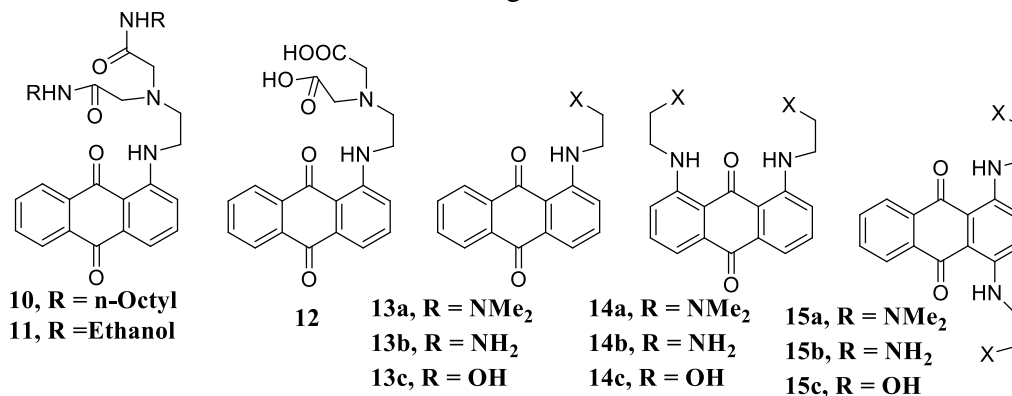


Figure 3. Receptor **10-15** used for sensing properties.

Ermakova and coworkers have reported the receptors **16a-b**, based on 1,8-diaminoanthraquinone derivatives containing phosphonic acid esters. Both receptors showed selective detection of Hg²⁺, as shown in figure 4. The receptor **16a** showed an absorbance band at 561 nm. It is due to ICT. The receptor showed an absorption peak at 56 nm. The absorption quenched with the appearance of a new peak at 509 nm on interacting with Hg²⁺ (5 equiv.), and blue color goes to pink in color. However, **16a** remains silent towards other metal salts. The receptor **16b** showed absorbance maxima at 565 nm. The intensities of absorption peak quenched, and the blue-violet color goes pink in color in the presence of Hg²⁺ (5 equiv.) [55]. On continuous work on amino-anthraquinone derivatives containing phosphonic acid esters, Guilard *et al.* reported water-soluble colorimetric chemosensor **17c-f**.

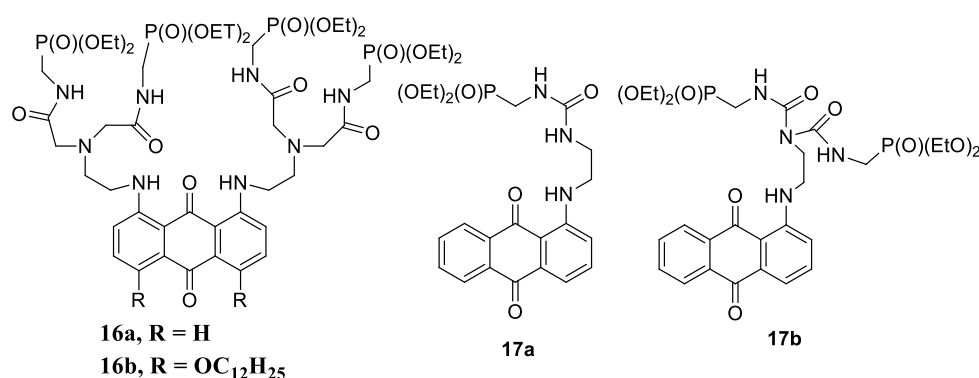


Figure 4. Receptor **16-17a-b** used for sensing properties.

All the synthesized receptors were able to detect Cu²⁺ over other metal salts and produced color change [52]. Anthraquinone unit has also been incorporated into the macrocyclic backbone to develop selective sensors resulting from additional coordination groups' simple attachment to the respective macrocycle. Guilard and his research group synthesized a series of 1,8-diaminoanthraquinone based poly-azamacrocycles **18** and **19a-b** and studied their cation binding affinities. Receptor **18** showed absorbance maxima at 562 nm.

The presence of Cu^{2+} to **18** showed a bathochromic shift ($\Delta\lambda = 94 \text{ nm}$) in its absorption band. In contrast, a hypsochromic shift ($\Delta\lambda = 26 \text{ nm}$) was observed upon the addition of Al^{3+} . The receptor **19a** detected Cu^{2+} and Pb^{2+} in DMSO- H_2O (1:1), showed color changes from violet to pink for Pb^{2+} and blue for Cu^{2+} .

On the other hand, for **19b**, the violet color turns to pink. The hypsochromic shift ($\Delta\lambda = 30 \text{ nm}$) in the presence of Pb^{2+} and a bathochromic shift ($\Delta\lambda = 103 \text{ nm}$), and the violet color turns to blue on the addition of Cu^{2+} . The authors attributed that the hypochromic shifts were raised due to the conformational changes. The bathochromic shift resulted from the deprotonation of the -NH of the receptor, as shown in figure 5 [56]. Kumar and coworkers have reported the metal ion sensing ability of quinone receptor **20** containing an N, N-dimethyl group [57]. Receptor **20** showed absorbance maxima at 436 nm. The absorption band's intensities quenched with the appearance of a new peak at 520 nm with a yellow-green color turn to pink in the presence of Cu^{2+} (10 equiv.). The authors attributed that the red shift of absorbance maxima was due to deprotonation of NH-amine, and quenched fluorescence occurred due to LMCT.

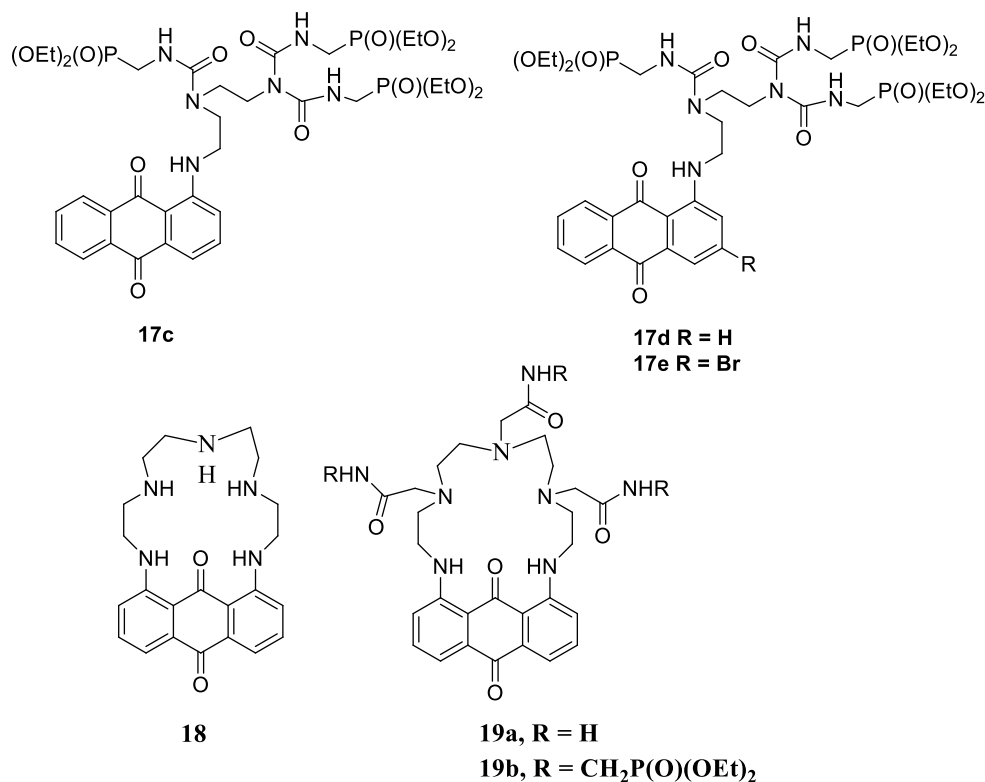


Figure 5. Receptor **17c-19** used for sensing properties.

Wu and his research group have reported a few amino-anthraquinone receptors **21-22** [58]. Both receptors were used for selective colorimetric chemosensor for various metal ions in CH_3OH : HEPES (4:1) using UV-vis spectra. In the presence of Cu^{2+} , a bathochromic shift ($\Delta\lambda = 76 \text{ nm}$ from 397 nm to 473 nm) yellow color solutions of **21-22** turn to dark-red. The bathochromic shifts are due to the deprotonation of -NH group of receptors. The receptor **21** remains silent towards other cations. Whereas Ni^{2+} to **22** ascribed a red shift of 86 nm and yellow color solutions turn to red. However, in the presence of Co^{2+} , **22** displayed a blue shift, and the yellow color turns to pale green. The authors found that receptor **22** did not respond to any color changes on treatment with group-IA, group-IIA, and other transition metal ions. 2-Methyl-1,4-naphthoquinone based chemosensor **23-24** selective detection of Cu^{2+} amongst various metal salts. This is attributed to the requisite of Cu^{2+} to -NH groups, which induce

deprotonation of -NH units to cause the observed color change. The same groups have reported the receptors **23** and **24** based on the pyridine scaffold capable of selectively binding Cu²⁺ ions [59] on continuous effort on colorimetric chemosensor. In UV-vis spectra, both receptors underwent a color change from orange to dark blue and a 168 nm red shift on the addition of Cu²⁺ as shown in figure 6.

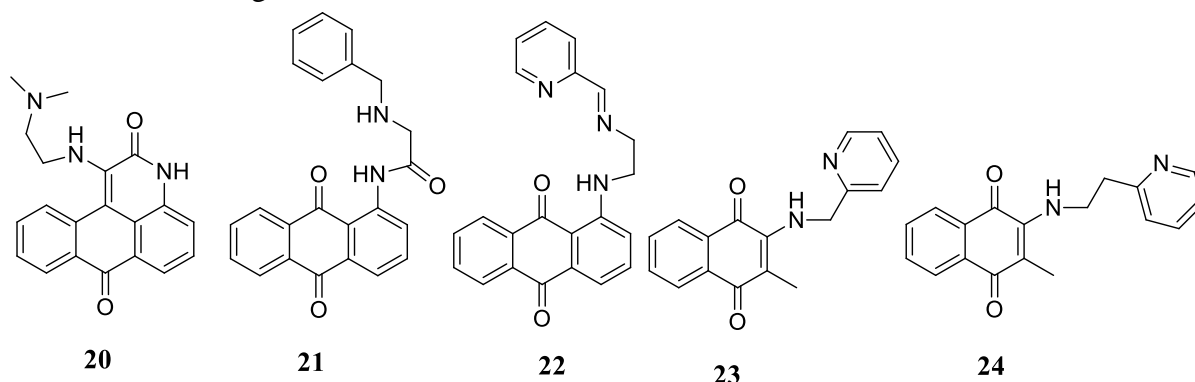


Figure 6. Receptor **20-24** used for sensing properties.

Yang *et al.* reported the cation sensing ability of a series of anthraquinone derivatives **25a-d** based on urea and thiourea group at 1,2-positions, as shown in figure 7 [60-61]. These derivatives exhibited naked eye visible color change in DMSO-CH₃CN (1:9, v/v) medium. With electron-withdrawing groups (such as NO₂) in **25a-b**, the color changes have occurred. UV-vis titrations showed that in the presence of Hg²⁺, **25a**, underwent a blue shift of 58 nm from absorption band 458 to 400 nm, and aurantium color changes to yellow. However, the absorption at 400 nm broadened. A new peak appeared at 650 nm in the presence of Ag⁺ and golden color changes orange-red. Kim and his research groups have reported receptors **26-27** to detect Cu²⁺ in ACN medium.

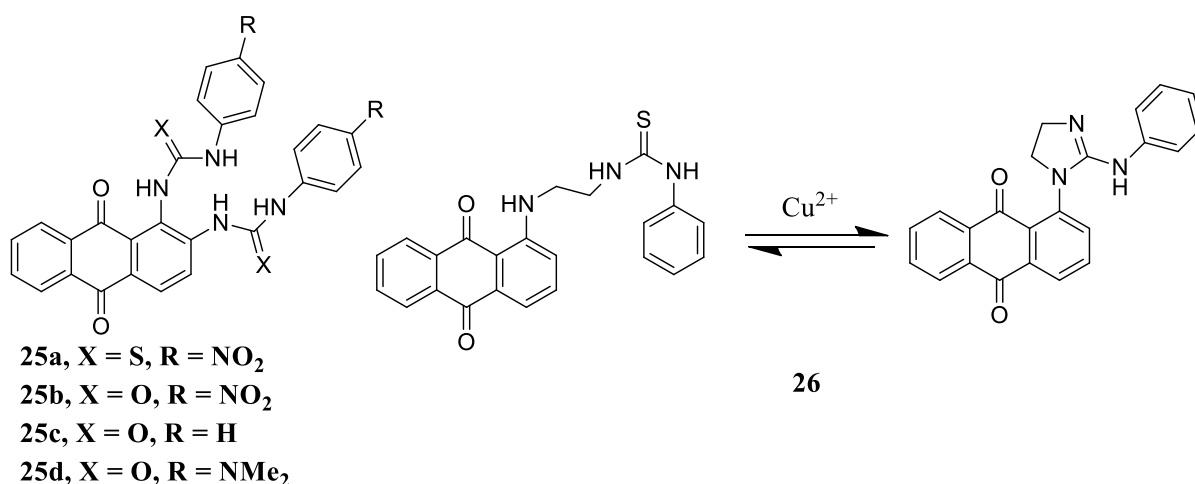


Figure 7. Receptor **25-26** used for sensing properties.

In UV-vis spectra, **131** displayed absorption maxima at 500 nm. The intensities of absorption quenched with the appearance of a new peak at 450 nm, and the red color solution of **26** goes to pale yellow. In fluorescence titration, in the presence of Cu²⁺ to the solution of **26**, resulting in a blue shift emission at 590 nm to 555 nm. The authors found that the blue shift is due to the desulfurization process. However, **27** showed a very weak fluorescence emission and on treatment with Cu²⁺ showed enhancement of fluorescence at 560 nm. Red color solutions change to yellow [62]. Anthraquinonoidalcalix-[4]-arene receptors **28a** selectively

recognized Zn^{2+} ions over other metal salts [63]. **28a** showed excellent selectivity for Zn^{2+} ions over other transition metal ions.

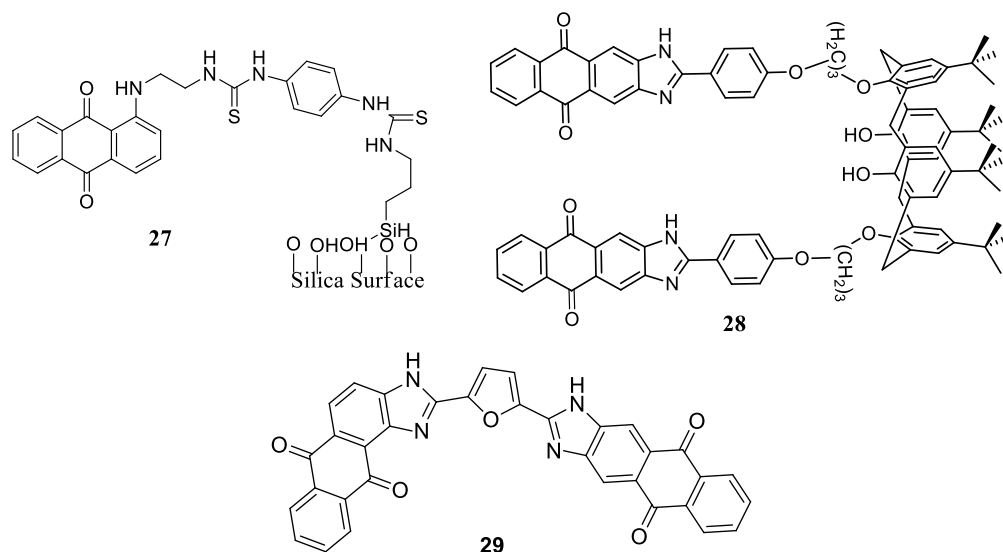


Figure 8. Receptor **27-29** used for sensing properties.

Kim and his research group described an anthraquinone tethered imidazole derivatives **29** [63]. Receptor **29** exhibited selective detection of Pd^{2+} and Pd^0 . The authors found that the selective detection of Pd^{2+} is due to the ligand to metal transition. In contrast, selective detection of Pd^0 occurred due to metal to ligand transition excitation, as shown in figure 8. Receptor (**30a-b**), based on an azacrown-anthraquinone derivative, showed detection of group-IA and group-IIA metal salts preferentially. Both receptors remain silent towards transition metal, a lanthanide metal, an actinide metal salts. Both receptors exhibited a very weak emission band at 515 nm. The weak fluorescence is due to the PET processes [64]. Kim and his research group designed an ESIPT based chemosensor receptor **31**, which showed selective and sensitive fluorescent change with In^{3+} , among other metal salts in CH_3CN solution. With the gradual addition of In^{3+} to **31**, the fluorescence emission peak quenched with the concomitant appearance of a new blue-shifted peak due to segregation of the intramolecular H-bond formation. The differential pulse CV studies were also conducted wherein the two cathodic peaks of **31** disappeared upon the addition of In^{3+} . An additional cathodic peak was observed from the reduction process of **31**: In^{3+} complex, as shown in figure 9 [65-66].

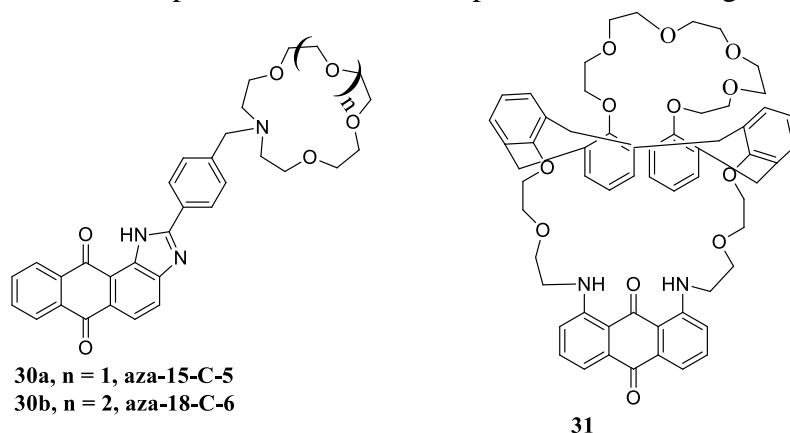


Figure 9. Receptor **30-31** used for sensing properties.

Receptor **32**, based on a zinc porphyrin-quinone linked derivative capable for selective detection Y^{3+} ions amongst other metal salts. The authors attributed that weak fluorescence of

32 was due to the electron-transfer from metal ions to **32** [67-68]. Gawali and his research group reported a series of bromine substituted amino-naphthoquinones (**33-37**) and examined their colorimetric sensing properties with various metal salts. The orange color turns to blue for **33** and dark green for **34** upon the addition of Cu^{2+} . This occurred due to deprotonation of -NH proton; however, receptors **35-37** remain silent towards other metal ions [69]. However, Elango *et al.* reported a naphthoquinone tethered amino triazole derivative **38**, which was selectively recognized as Hg^{2+} ions. The receptor showed absorption maxima at 445 nm. It is due to $n-\pi^*$ transition. In the presence of Hg^{2+} , the absorption intensities gradually quenched, and a new peak appeared at 569 nm.

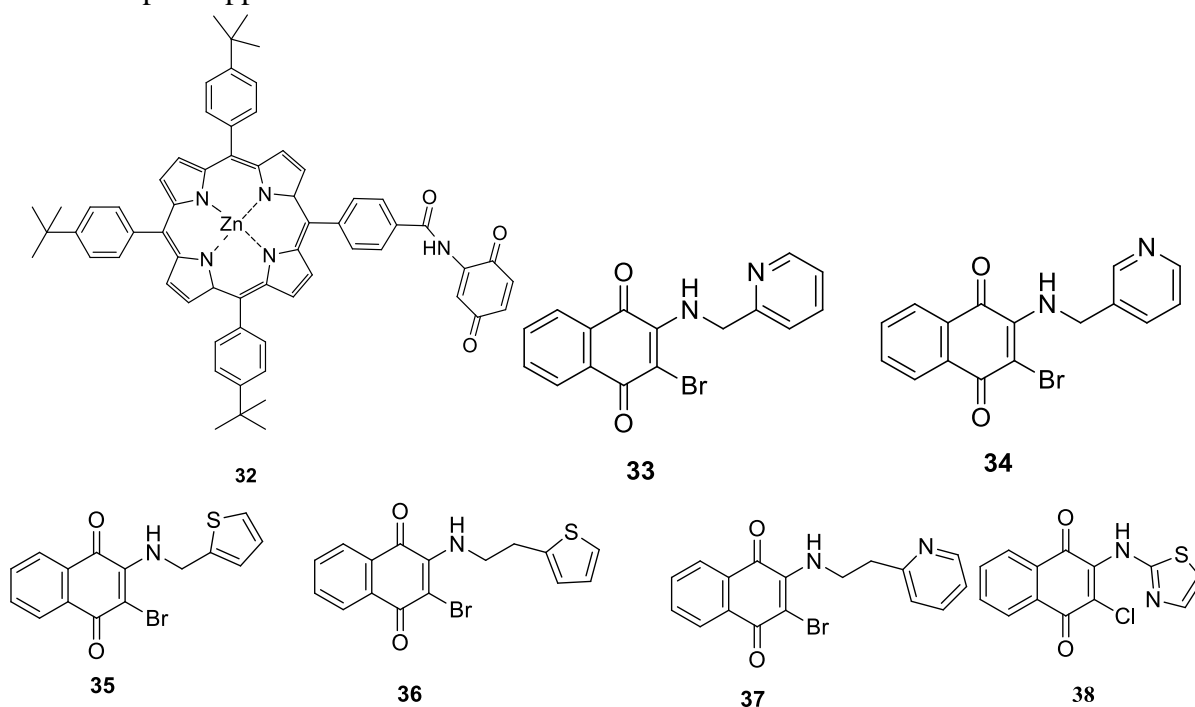


Figure 10. Receptor **32-38** used for sensing properties.

With the gradual addition of Hg^{2+} to **38**, an isosbestic point at 483 nm has appeared. It caused the color change from pale brown to blue. The fluorescence titrations showed the receptor form a 1: 1 complex with Hg^{2+} with moderate binding constant $K_a = 3.5 \times 10^4 \text{ M}^{-1}$. The detection limit was found to be $0.3 \mu\text{M}$. The authors found that the receptor was selectively recognized Hg^{2+} ions, which was lower than the permissible limit in the drinking water given by WHO [69] in figure 10. Baruah *et al.* reported a series of pyridine tethered 1,4-naphthoquinone derivatives (**39-42**) and exhibited their sensing properties by using UV-vis and fluorescence titrations, as shown in figure 11.

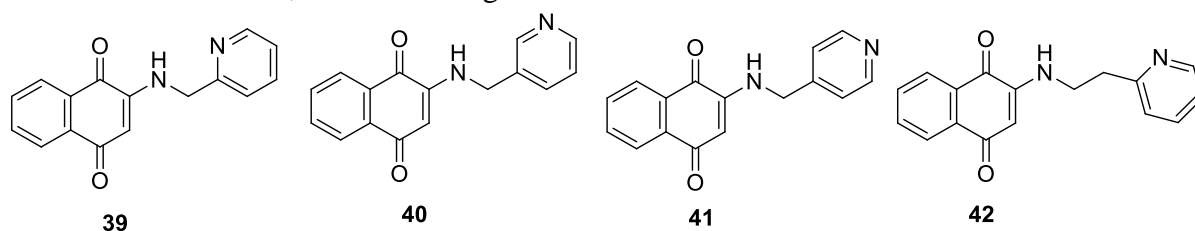


Figure 11. Receptor **39-42** used for sensing properties.

Receptor **39** displayed absorption maxima at 438 nm in methanol. Upon excitation, 445 nm emission peak appeared at 538 nm, which was attributed to $\pi^*-\pi$. **39** showed high selectivity

towards Mn^{2+} ions. However, receptor **40** showed highly selective for Cd^{2+} ions (OFF-ON-ON) over other metal ions. It is due to the interaction between Cd^{2+} ions and **40** [70].

2.2. Alkoxy based receptors.

Wang and his research groups have reported a Cu^{2+} sensor by forming an inclusion complex of **43** with β -CD in an aqueous medium [71]. The aqueous solution of receptor **43** envisages three distinct forms - the yellow color in a neutral medium; pink in dilute alkali (due to anionic state). In the case of a strong alkali medium (due to di-anionic state), shows deep blue color was observed in aqueous media. The authors found that the absorption and fluorescence intensities of **43** were enhanced by β -CD. The presence of ammonia molecule, the **43**: β -CD complex, showed selective toward Cu^{2+} ions amongst other cations. It resulted in color change, and chelation enhanced quenching (CHEQ). The presence of lone pair of an electron in a nitrogen atom plays an important role in the formation of the complex with Cu^{2+} besides **43** as shown in figure 12. The authors demonstrated that the **43**- Cu^{2+} complex was formed by binding through the carbonyl ($-C=O$) and O-atom of hydroxyl unit ($-OH$) and two ammonia molecules. Thus, ammonia acted as both bases as well as a ligand. It was applicable for the determination of Cu^{2+} in tap and river water samples and in tea. Kar and coworkers [72] used alkoxy-anthraquinone-based receptors **44a-b** for selective recognition of alkali earth metals (Group-IIA), amongst other metal ions. Both receptors showed absorbance maxima at 278 nm and 427 nm, respectively. The absorption band at 427 nm was raised because of charge transfer from $-OH$ or $-OCH_3$ (donor) units to anthraquinone (acceptor) unit. In the presence of Mg^{2+} , a new absorption band was raised in 500-575 nm, and the yellow color turns to red. The color and spectral change occurred due to the formation of complexes between the metal and receptors.

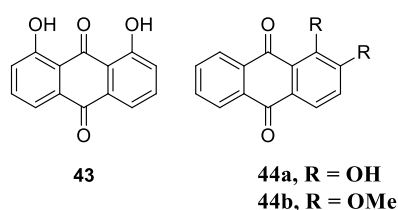


Figure 12. Receptor **43-44** used for sensing properties.

Shamsipur and coworkers have studied the role of Cu^{2+} ions in anthraquinone derivatives **45** by using UV-vis and fluorescence titrations [73]. Receptor **45** was used for the selective detection of Cu^{2+} ions in black tea samples. Similarly, diester-anthraquinone conjugate receptor **46** for selective detection of Li^+ and Na^+ ions over other metal salts was reported by Jeon *et al.* The authors found that the derivative showed red shift for Li^+ and Na^+ [74]. 9,10-anthraquinone based 2-aminothiophenol derived receptors **47a-b** were found to be selective Cu^{2+} reported by Kaur *et al.* in the presence of Cu^{2+} , **47b** showed a new absorption band around 520-800 nm with light yellow color turns to brown. The addition of divalent cations did not affect the absorption spectrum of **47b**. This indicates that the presence of NH_2 is a requirement to form a chelated complex to show the change in color by this series of the receptor [75]. Sykes and coworkers [76] developed a Cu^{2+} and Fe^{3+} sensor **48**. The addition of Cu^{2+} or Fe^{3+} to **48** led to a 20 fold enrichment of fluorescence emission, resulting in red-orange fluorescence color. It is due to the formation of **49**. The same groups have also designed and synthesized a series of anthraquinone containing cyclic and acyclic polyether receptors 50-52

[77-78] on continuous effort on cation sensing. All synthesized receptors governed 1:1 complexes with hydronium ion, as shown in figure 13.

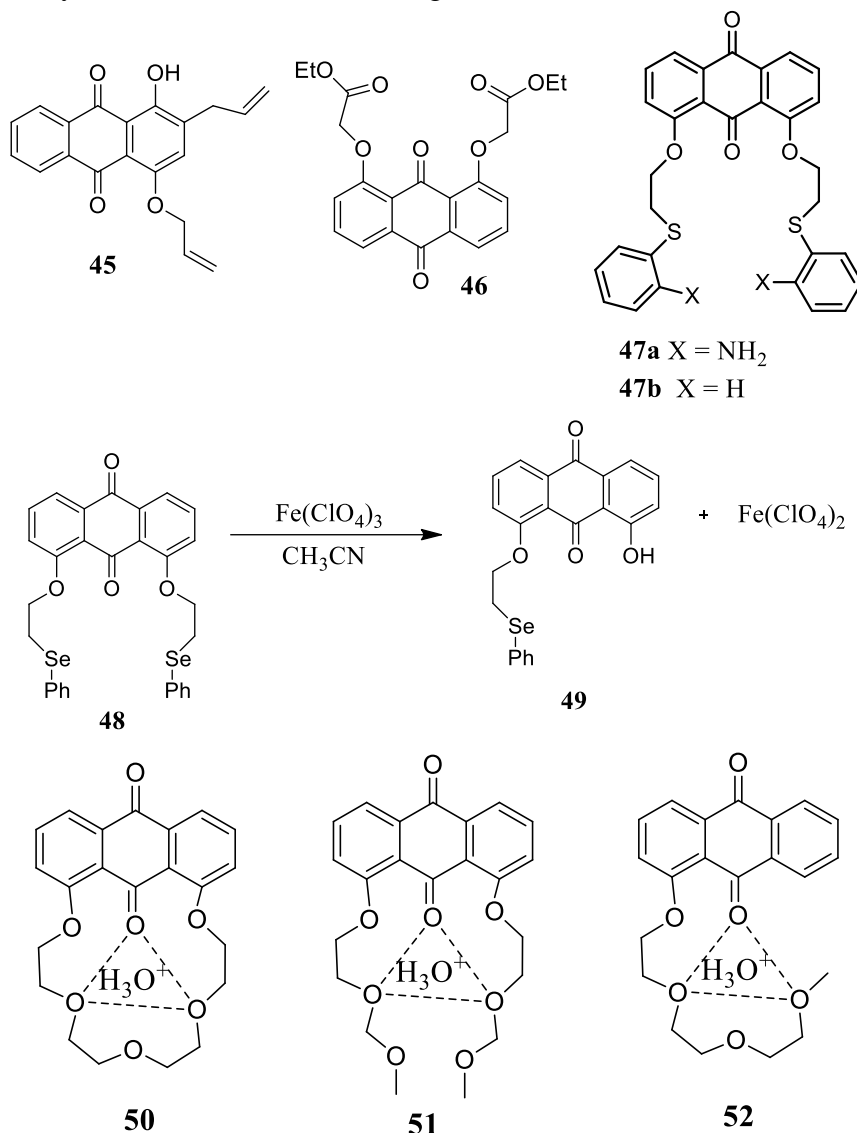


Figure 13. Receptor 45-52 used for sensing properties.

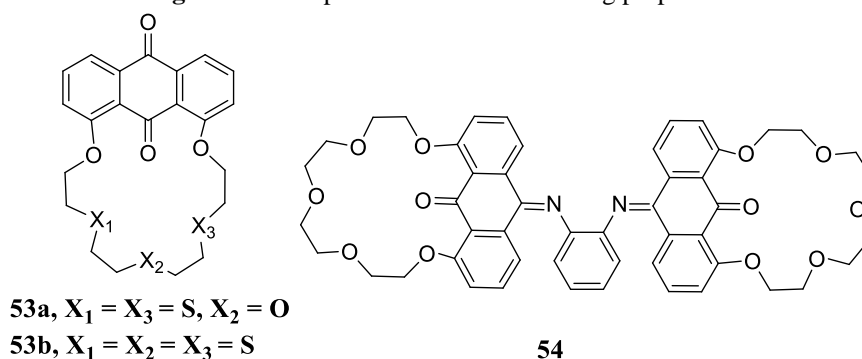


Figure 14. Receptor 53-54 used for sensing properties.

The receptor **50** displayed selective sensing of Pb²⁺ and Ca²⁺ in acetonitrile solution. Upon addition of Pb(ClO₄)₂ and Ca(ClO₄)₂, **50** displayed bathochromic shift ($\Delta\lambda = 20$ nm) from absorption band 380 to 400 nm. The bathochromic shift was raised due to the replacement of non-radiative transitions by radiative transitions. Sykes and his research groups have also reported sulfur-containing anthraquinone derivatives **53a-b** and examined their metal ion sensing properties in acetonitrile solution using UV-vis spectra, as shown in figure 14 [79].

The authors found that both receptors were used for selective recognition of Cd^{2+} and Hg^{2+} in acetonitrile. The receptor **53a** showed a bathochromic shift ($\Delta\lambda = 14$ nm) from absorption band 388 to 402 nm on the addition of Cd^{2+} , and the emission band occurred at 506 nm on reacting with Cd^{2+} ions.

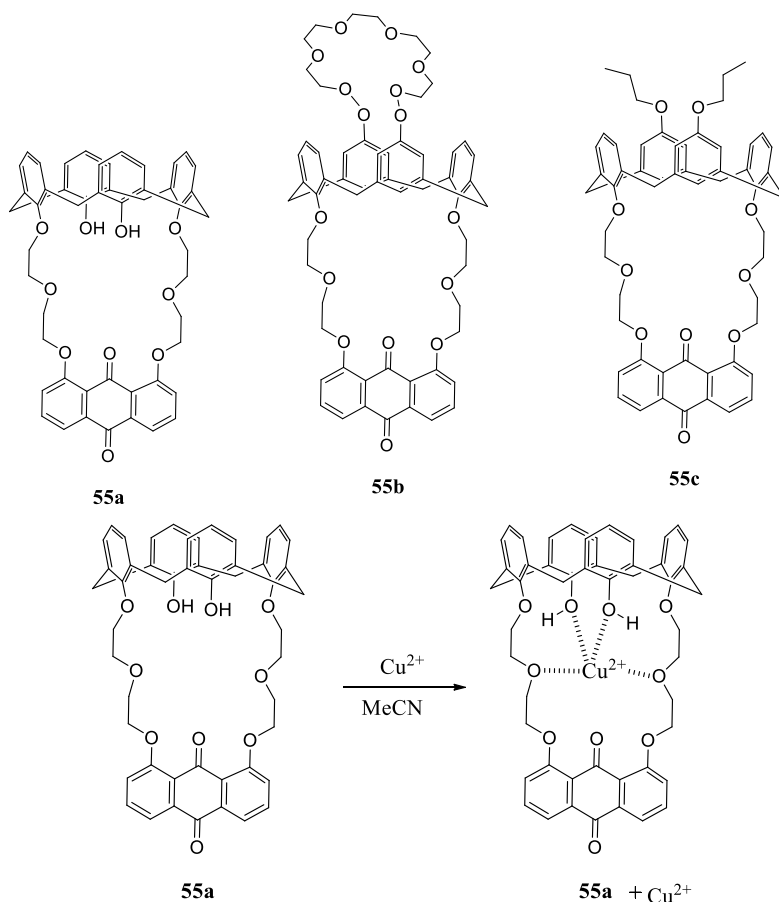


Figure 15. Receptor **55 a-c** used for sensing properties.

However, the receptor **53b** showed a bathochromic shift ($\Delta\lambda = 16$ nm) from the absorption band 390 to 406 nm on the addition of Hg^{2+} ion. The enhancement fluorescence was observed at 520 nm was observed in the presence of Hg^{2+} ions. In another case, the same research group also reported a potent molecular probe **54**, as shown in figure 14, which was selective detection of Ba^{2+} , amongst other metal ions. Coordination of Ba^{2+} ions to nitrogen atom lone pairs restricted the rotation around the C=N groups, thus, inhibiting the isomerization and consequent activation of the luminescence resulting in enhanced emission [80]. Calix-[4]-anthraquinone receptor **55a-c** was used for selective recognition of Cu^{2+} ions amongst other metal ions. **55a** showed bathochromic shift 70 nm, and yellow color solutions go to red color in the presence of Cu^{2+} ions in acetonitrile solution. The authors suggested that ICT played an important role in forming complexes between **55a** and Cu^{2+} ions [81]. Receptors **55b-c** did not respond to any color change and spectral change towards Cu^{2+} and other cations due to the absence of two proximal -OH groups, as shown in figure 15.

They have also reported an anthraquinone based receptor **56** possessing 1,2,3-triazoles; the receptor was used to detect Al^{3+} over other metal ions [82]. The addition of Al^{3+} ions to **56** showed a bathochromic shift of 120 nm. From the fluorescence profile, enhancement of fluorescence was observed in the presence of Al^{3+} . The bathochromic shift and enhanced fluorescence occurred due to ICT and chelation enhanced fluorescence. It resulted as Al^{3+} led complex with **160**.

On the other hand, receptor **57** was capable of detecting Cu^{2+} . In the presence of Cu^{2+} , a bathochromic shift of 70 nm was observed. The quenched fluorescence was occurred due to the paramagnetic nature of Cu^{2+} [83].

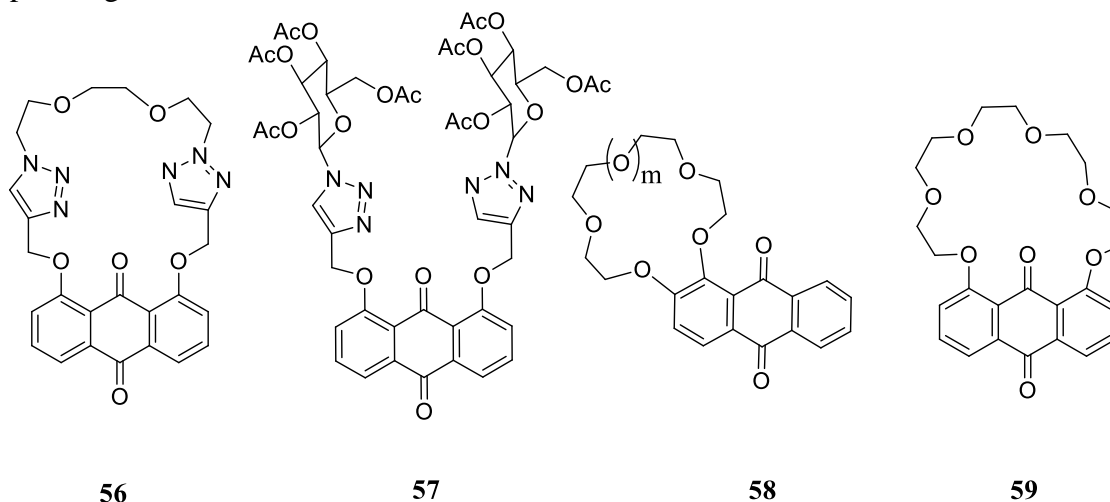


Figure 16. Receptor **56-59** used for sensing properties.

Erkand and his coworkers have reported anthraquinone-based receptors **58-59**, which were capable of binding Li^+ over other metal salts. Receptor **59** showed absorption bands at 373 nm and 333 nm in the presence of Li^+ . The authors suggested that the absorption peak at 373 nm due to a free receptor and 333 nm is due to its cationic complex. The binding ability of metal salts towards receptors completely depends on the cation radius and macrocycle size. 1,8-macrocyclic-9,10-anthraquinone derivative **59** showed a small complexing effect using the UV-vis spectra absorption at 383 nm, probably due to the carbonyl's hindering role groups, as shown in figure 16 [84].

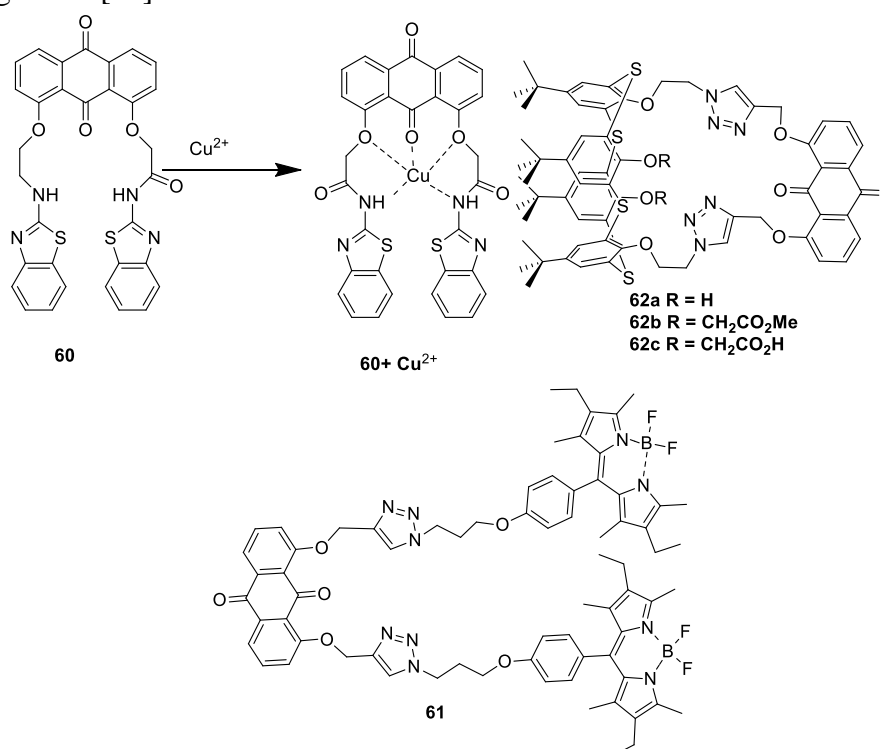


Figure 17. Receptor **60-62** used for sensing properties.

Ghosh and his coworkers have reported an anthraquinone-based molecular receptor **60** for selective detection of Cu^{2+} ions using fluorescence titration. Upon excited at 380 nm, the

emission band was raised at 457 nm. The addition of Cu^{2+} ions to **60**, gradually quenched the fluorescence emission with a blue shift of 25 nm. The authors found that the receptor **60** form 1:1 complex with Cu^{2+} ions with an association constant of $1.77 \times 10^4 \text{ M}^{-1}$. On the other hand, receptor **60** remains silent towards other metal salts [85].

Kursunlu reported a novel triazole tethered Bidipy-anthraquinone receptor **61**, as shown in figure 17. For selective detection of Al^{3+} ions over other metal salts. The receptor showed an absorption band at 212, 290, 400, and 513 nm. The band was observed at 400 nm due to $\pi-\pi^*$ transitions of anthraquinone and Bodipy groups. Upon addition of 20 equiv. of Al^{3+} ions to **61**, the absorption peak shifted around at 290 and 400 nm. However, receptor **61** remains silent in the presence of other metal salts. The authors attributed that the selective of Al^{3+} due to charge transfer from bodily groups to anthraquinone-triazole moiety [86-87]. Gou *et al.* [88] have reported a series of thiacalix[4]pseudo crown receptors (**62a-c**) bearing naphthoquinone function for the detection of various metal salts by using UV-vis and fluorescence titrations. From the UV-vis spectra, it was observed that the receptor **62a** and **62b** showed absorption bands at 372 and 376 nm, respectively. It is due to anthraquinone moiety. The receptor **62a** showed a weak fluorescence emission band at 427 nm upon excitation at 375 nm. Upon addition of Pb^{2+} ions, fluorescence enhancement occurred along with a new band raised at 465 nm. The red shift of emission fluorescence was due to ICT mechanism. Under the ideal condition, the receptor remains silent towards other metal salts. From Job's plot, it was observed that receptor form 1: 1 complex with Pb^{2+} ions. The authors found that the Pb^{2+} ions strongly interact with the carbonyl group's oxygen and N-atom of the triazole group. Conversely, receptor **62b** showed an emission band at 428 nm upon excitation at 375 nm. Receptor **62b** showed similar behavior towards Pb^{2+} . However, on the addition of Zn^{2+} to the receptor, fluorescence enhancement (3.75 fold) was perceived. A new band occurred at a higher wavelength at 476 nm. The binding constant measurement showed that the receptor formed 1: 1 complex with Zn^{2+} ions. The receptor remains silent towards other metal salts.

2.3. Pentaquinones based receptors.

A series of pentaquinone-based receptors were synthesized by Bhalla and his research group. They exhibited their sensing properties by using UV-vis and Fluorescence spectroscopy. Thiophene tethered pentaquinone receptor **63** exhibited selective and sensitive binding affinities toward Fe^{3+} and various nitro-aromatics. In THF- H_2O (1: 9 v/v), receptor **63** showed absorbance maxima at 415 nm, 328 nm, and 300 nm, respectively. In the presence of water, the absorption band intensity increased due to the formation of aggregates of receptor **63**. Upon excitation at 328 nm, receptor **63** showed the emission band at 560 nm. The presence of Fe^{3+} to **63** leads to quenching the fluorescence emission at 560 nm [89].

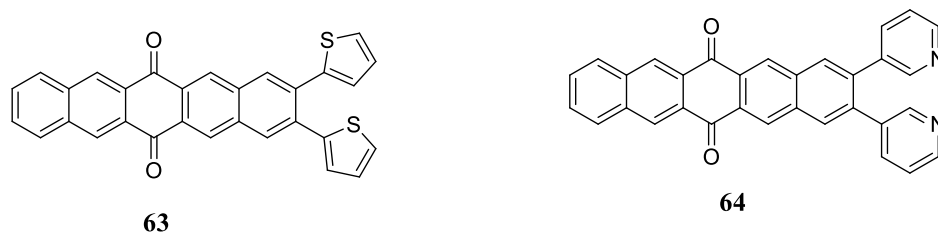


Figure 18. Receptor **63-64** used for sensing properties.

The authors found that receptor **63** used to detect Fe^{3+} in water, and also in the presence of blood serum milieu. The same groups have also reported nanoaggregates of pentaquinone

receptor **64** and examined its sensing behavior towards Pd^{2+} . **64** displayed the enhancement of the absorption band, followed by quenching the fluorescence intensity. It is occurred due to the formation of a complex between **64** and Pd^{2+} with nanoaggregates of **64** as shown in figure 18 [90].

Similarly, the same groups have also reported a series of pentaquinone based receptors **65-66** (Figure 19) to recognize various metal salts by using UV-vis and fluorescence spectroscopy. In THF- H_2O (9: 1), receptor **65** showed an absorption band at 298 and 403 nm. Receptor **65** underwent hypsochromic shifts in the presence of Hg^{2+} . The enhancement of fluorescence has occurred in the presence of Hg^{2+} . In the presence of Hg^{2+} **65** was hydrolyzed and led the fluorescent product **66** [91]. Both receptors were used to detect Hg^{2+} in blood serum and prostate cancer cell lines.

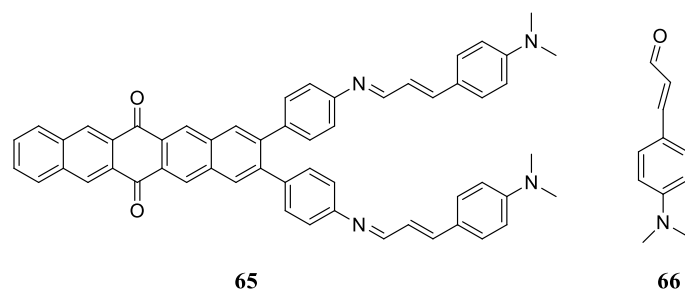


Figure 19. Receptor **65-66** used for sensing properties.

Receptor **67a** showed weak fluorescence emission at 500 nm upon excitation at 390 nm. In THF, **67a** showed enhancement fluorescence upon addition of 1 equiv. of Zn^{2+} due to the formation of a complex between **67a** and Zn^{2+} . A similar trend was observed for **67b** [92]. Receptor **68** (Figure 20) endorsed the Zn^{2+} ions under F^- ions triggered a synergistic effect. **68** underwent a fragile fluorescent intensity at 530 nm upon irradiation 350 nm. In the presence of Zn^{2+} , gradual enhancement of fluorescence intensity was observed. The enhancement of fluorescence emission is due to the formation of the complex between them. The detection limit was calculated from the fluorescence profile and found to be 30 nM [93].

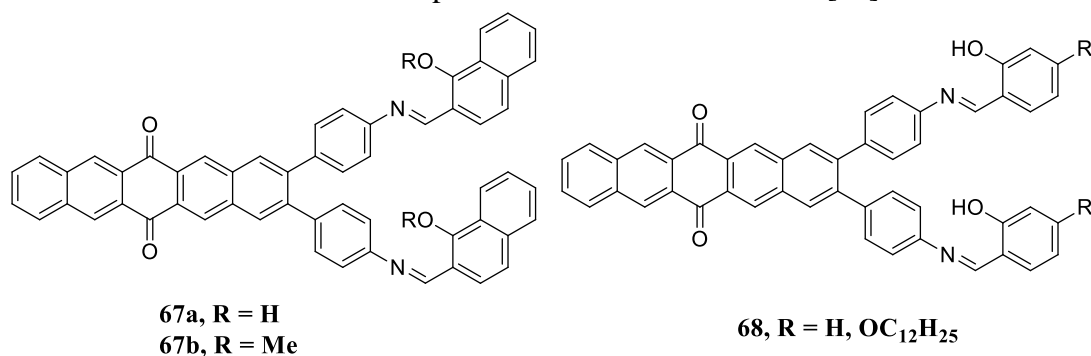


Figure 20. Receptor **67-68** used for sensing properties.

DMSO **69** showed hypsochromic shifts along with a new band that occurred at 443 nm. The authors found that the hypsochromic absorption band occurred due to the formation of deprotonated species **70** with F^- ions. Absorption band occurred at 443 nm disappeared, and absorption intensities at 311 nm increase in the presence of Cu^{2+} , due to the formation of complex **71** [94]. On continued effort on pentaquinone derivatives, the same group reported the rhodamine appended pentaquinone **72** and **73** (Figure 21). Both receptors were used to detect Hg^{2+} . Upon excitation at 360 nm, receptors showed the emission band at around 572-582 nm on the addition of Hg^{2+} . It caused the opening of the Spiro lactam ring [95].

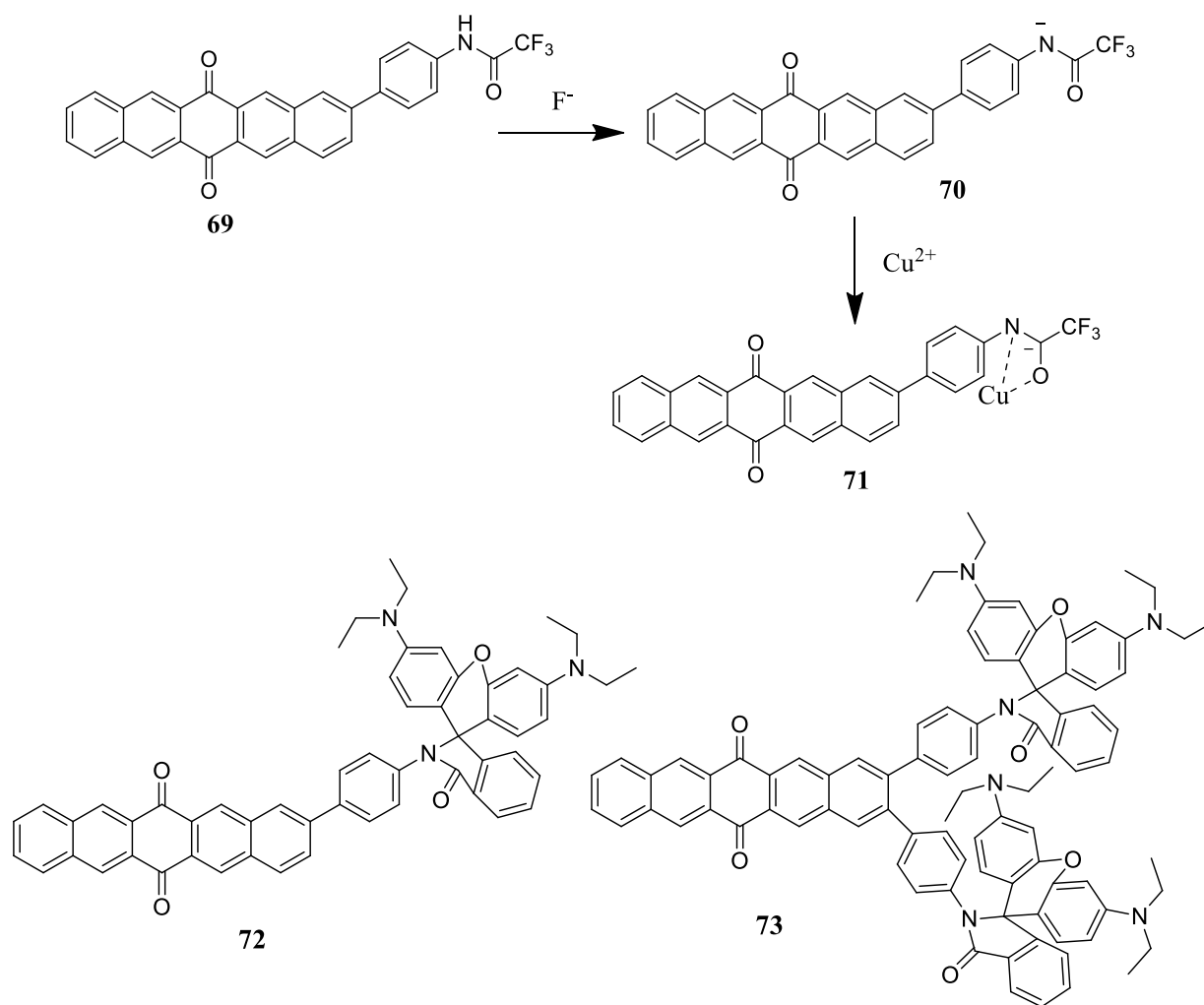


Figure 21. Receptor **69-73** used for sensing properties.

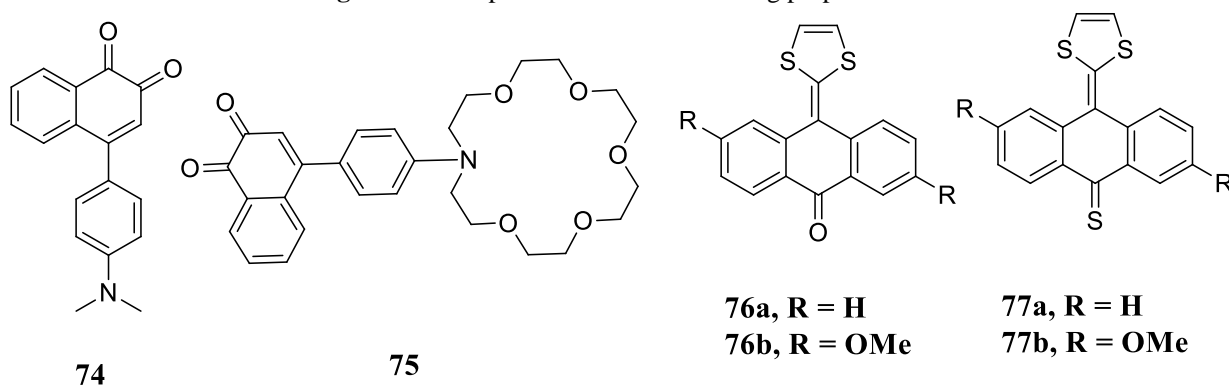


Figure 22. Receptor **74-77** used for sensing properties.

2.4. Miscellaneous quinone based receptors.

Highly colored 1,2-naphthoquinone based receptors **74-75** (Figure 22) based on the crown ether group were used as chromogenic chemosensors for metal cations in ACN was reported by Soto and his research group. Both receptors showed absorption intensities at 534 and 532 nm. It was responsible for an intra-ligand charge transfer band involving the amine and the carbonyl groups of receptors. Receptor **74** was selectively recognized Cu^{2+} and Fe^{3+} , amongst other metal ions. On the other hand, receptor **75** showed similar behaviors to **74** [40].

Receptors **76a-b** and **77a-b** were used for selective recognition of Hg^{2+} , Cu^{2+} and Fe^{3+} , respectively. The absorption intensities at 579 nm quenched along with a new band appeared

at 263 nm in the presence of Hg^{2+} and Cu^{2+} ions. It caused the color change from dark-blue to orange. However, **76a** was used to detect Cu^{2+} and Fe^{3+} [96]. Zhu and his research groups have conveyed an ICT based receptor **78** for the selective recognition of thiol and the metal ions Zn^{2+} and Co^{2+} in $\text{CH}_3\text{CN}-\text{H}_2\text{O}$. From the UV-vis profile, it was found that the absorption intensities decreased with the appearance of a new absorption band at 394 nm in the presence of Zn^{2+} and Co^{2+} [97].

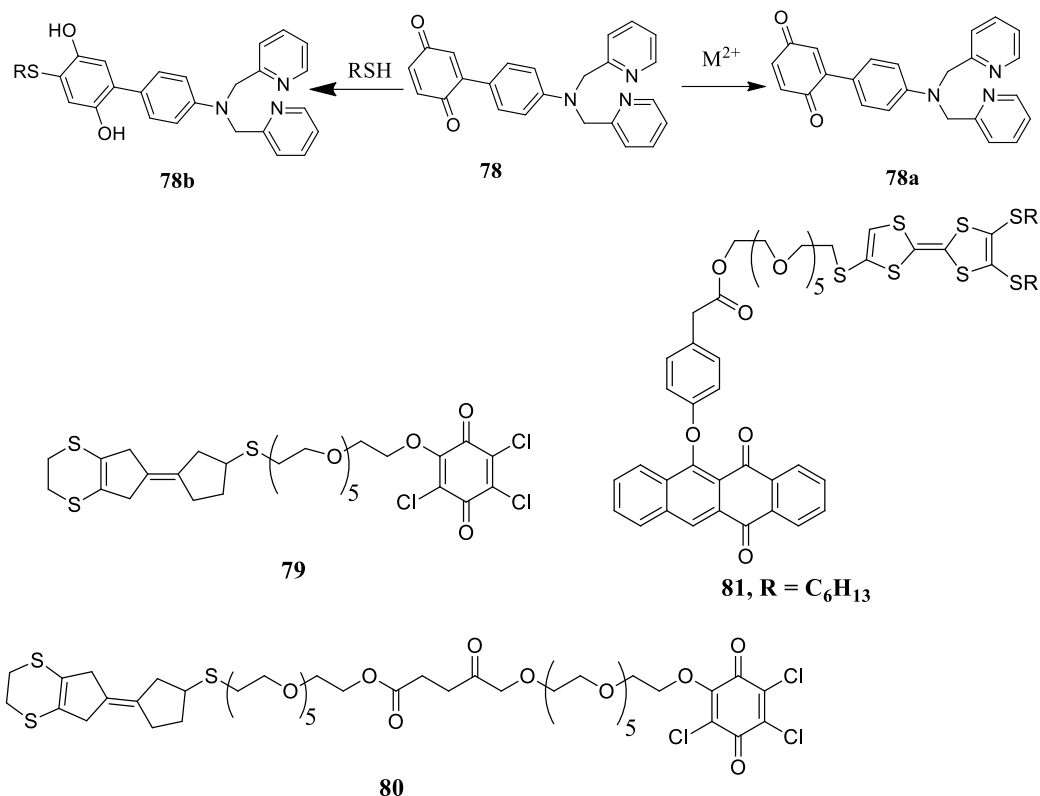


Figure 23. Receptor **78-81** used for sensing properties.

Zhang *et al.* described phenoxy-quinone the third tetrathiafulvalene derivatives **79-81** (Figure 23) for the sensing of Pb^{2+} , Sc^{3+} , and Zn^{2+} , respectively [98]. From the UV-vis titrations, it was found that the absorption intensities decreased with the appearance of a set of new absorption bands at 450 and 845 nm. It is due to the electron transfer from TTF to quinone moiety. In UV-vis spectra, receptor **81** displayed the absorption bands at 450 and 479 nm, respectively. The authors found that in case of the dark condition, **81** remains silent towards various metal ions; however, in the presence of light, the intensities of absorption band quenched with the appearance of a new absorption band at 790 nm in the presence of various metal ions such as Pb^{2+} , Sc^{3+} , and Zn^{2+} , respectively. It is due to the formation of TTF^+ .

3. Conclusions

Fluorescence and colorimetric chemo-sensorial chemistry has grown noticeably after the Nobel Prize in Supramolecular Chemistry to Charles J. Pedersen, Jean-Marie Lehn, and Donald J. Cram. In this review, we have given an overview of the developments of fluorescent and colorimetric indicators built on the quinone scaffold. All the colorimetric and fluorescent sensors were divided into various categories according to their receptors. The results summarized in this review show a clear idea about the important factors such as acceptor-donor; size and flexibility piece a noteworthy role in colorimetric and fluorescent sensors, more efficiency and efficacy for detecting specific analytes. We hope this review showed a

significant role in developing new potent molecular probes for any analytes from cations to anions and small biomolecules that need to be detected, monitored, and visualized. Since quinones already offer an outstanding fluorophores platform. We strongly believe that this research area will become more active due to the biological and environmental implications of various metal salts and anions. Further investigations will continue to increase.

Funding

Dr. Jali acknowledges a fund from DST, India, by EMEQ project (No.-EEQ/2019/000091). The authors also thank the Department of Chemistry, VSSUT, Burla for providing a research facility.

Acknowledgments

Dr. Jali thank the Department of Chemistry, VSSUT, Burla for providing a research facility.

Conflicts of Interest

The authors have declared that no competing interests exist.

References

1. Guo, C.; Sedgwick, A.C.; Hiaro, T.; Sessler, J.L. Supramolecular fluorescent sensors: An historical overview and update. *Coord. Chem. Rev.* **2021**, *427*, <https://doi.org/10.1016/j.ccr.2020.213560>.
2. Valeur, B.; Leray, I. Design principles of fluorescent molecular sensors for cation recognition. *Coord. Chem. Rev.* **2000**, *205*, 3-40, [https://doi.org/10.1016/S0010-8545\(00\)00246-0](https://doi.org/10.1016/S0010-8545(00)00246-0).
3. Lehn, J.M.; Eliseev, A.V. Dynamic Combinatorial Chemistry. *Science* **2001**, *291*, 2331-2332, <https://doi.org/10.1126/science.1060066>.
4. Chen, Li.; Liu, D.; Peng, J.; Du, Q.; He, H. Ratiometric fluorescence sensing of metal-organic frameworks: Tactics and perspectives. *Coord. Chem. Rev.* **2020**, *404*, <https://doi.org/10.1016/j.ccr.2019.213113>.
5. Thangadurai, T.D.; Nithya, I.; Rakkiyanasamy, A. Development of three ways molecular logic gate based on water soluble phenazine fluorescent 'selective ion' sensor, *Spectrochim. Acta A.* **2019**, *211*, 132-140, <https://doi.org/10.1016/j.saa.2018.12.006>.
6. Naha, S.; Varalakshmi, A.; Velmathi, S. Nanomolar colorimetric hypochlorite sensor in water. *Spectrochim. Acta A.* **2019**, *220*, <https://doi.org/10.1016/j.saa.2019.05.028>.
7. Pandey, R.; Kumar, A.; Xu, Q.; Pandey, D.S. Zinc(ii), copper(ii) and cadmium(ii) complexes as fluorescent chemosensors for cations. *Dalton Trans.* **2020**, *49*, 542-568, <https://doi.org/10.1039/C9DT03017D>.
8. Lochman, L.; Machacek, M.; Miletin, M.; Uhlřřova, Š.; Lang, K.; Kirakci, K.; Zimcik, P.; Novakova V. Red-Emitting Fluorescence Sensors for Metal Cations: The Role of Counteranions and Sensing of SCN⁻ in Biological Materials. *ACS Sens.* **2019**, *4*, 1552–1559, <https://doi.org/10.1021/acssensors.9b00081>.
9. Zhang, N.; Zhang, D.; Zhao, J.; Xia, Z. Fabrication of a dual-emitting dye-encapsulated metal-organic framework as a stable fluorescent sensor for metal ion detection. *Dalton Trans.* **2019**, *48*, 6794-6799, <https://doi.org/10.1039/C9DT01125K>.
10. Li, H.Y.; Zhao, S.N.; Zang, S.Q.; Li, J. Functional metal–organic frameworks as effective sensors of gases and volatile compounds. *Chem. Soc. Rev.*, **2020**, *49*, 6364-6401, <https://doi.org/10.1039/C9CS00778D>.
11. Li, M.; Cui, Z.; Pang, S.; Meng, L.; Ma, D.; Shi, Z.; Feng, S. Luminescent covalent organic framework as a recyclable turn-off fluorescent sensor for cations and anions in aqueous solution. *J. Mater. Chem. C* **2019**, *7*, 11919-11925, <https://doi.org/10.1039/C9TC03265G>.
12. Ye, F.; Wu, N.; Li, P.; Liu, Y.L.; Li, S.J.; Fu, Y. A lysosome-targetable fluorescent probe for imaging trivalent cations Fe³⁺, Al³⁺ and Cr³⁺ in living cells. *Spectrochim. Acta A.* **2019**, *222*, <https://doi.org/10.1016/j.saa.2019.117242>.
13. Bayindir, S.; Toprak, M. A novel pyrene-based selective colorimetric and ratiometric turn-on sensing for copper. *Spectrochim. Acta A.* **2019**, *213*, 6-11, <https://doi.org/10.1016/j.saa.2019.01.053>.
14. Bayindir, S. A simple rhodanine-based fluorescent sensor for mercury and copper: The recognition of Hg²⁺ in aqueous solution, and Hg²⁺/Cu²⁺ in organic solvent. *J. Photochem. Photobiol. A.* **2019**, *372*, 235-244, <https://doi.org/10.1016/j.jphotochem.2018.12.021>.
15. Kamaci, M.; Kaya, I. Polymeric fluorescent film sensor based on poly(azomethine-urethane): Ion sensing and surface properties. *React Funct Polym* **2019**, *136*, 1-8, <https://doi.org/10.1016/j.reactfunctpolym.2018.12.021>.

16. Podasca, V.E.; Chibac, A.L.; Buruiana, E.C. Fluorescence quenching study of a block copolymer with uracil end units by means of nitroaromatic derivatives and metal cations. *J. Mol. Liq.* **2019**, *292*, <https://doi.org/10.1016/j.molliq.2019.111385>.
17. Jiang, P.; Guo, Z. Fluorescent detection of zinc in biological systems: recent development on the design of chemosensors and biosensors. *Coord. Chem. Rev.* **2004**, *248*, 205-229, <https://doi.org/10.1016/j.cct.2003.10.013>.
18. Nolan, E.M.; Lippard, S.J. Tools and Tactics for the Optical Detection of Mercuric Ion. *Chem. Rev.* **2008**, *108*, 3443-3480, <https://doi.org/10.1021/cr068000q>.
19. Valeur, B.; Leray, I. Design principles of fluorescent molecular sensors for cation recognition. *Coord. Chem. Rev.* **2000**, *205*, 3-40, [https://doi.org/10.1016/S0010-8545\(00\)00246-0](https://doi.org/10.1016/S0010-8545(00)00246-0).
20. Rogers, C.W.; Wolf, M.O. Luminescent molecular sensors based on analyte coordination to transition-metal complexes. *Coord. Chem. Rev.* **2002**, *233*, 341-350, [https://doi.org/10.1016/S0010-8545\(02\)00023-1](https://doi.org/10.1016/S0010-8545(02)00023-1).
21. Chae, M.Y.; Czarnik, A.W. Fluorometric chemodosimetry. Mercury (II) and silver (I) indication in water via enhanced fluorescence signaling. *J. Am. Chem. Soc.* **1992**, *114*, 9704-9705, <https://doi.org/10.1021/ja00050a085>.
22. Bell, T.W.; Hext, N.M. Supramolecular optical chemosensors for organic analytes. *Chem. Soc. Rev.* **2004**, *33*, 589-598, <https://doi.org/10.1039/B207182G>.
23. Martínez-Mánez, R.; Sancenón, F. Fluorogenic and Chromogenic Chemosensors and Reagents for Anions. *Chem. Rev.* **2003**, *103*, 4419-4476, <https://doi.org/10.1021/cr010421e>.
24. Zhou, Y.; Zhang, J.F.; Yoon, J. Fluorescence and colorimetric chemosensors for fluoride-ion detection. *Chem. Rev.* **2014**, *114*, 5511-5571, <https://doi.org/10.1021/cr400352m>.
25. Chen, X.; Pradhan, T.; Wang, F.; Kim, J.S.; Yoon, J. Fluorescent chemosensors based on spiroring-opening of xanthenes and related derivatives. *Chem. Rev.* **2012**, *112*, 1910-1956, <https://doi.org/10.1021/cr200201z>.
26. Kumar, R.; Sharma, A.; Singh, H.; Suating, P.; Kim, H.S.; Sunwoo, K.; Shim, I.; Gibb, B.C.; Kim, J.S. Revisiting Fluorescent Calixarenes: From Molecular Sensors to Smart Materials. *Chem. Rev.* **2019**, *119*, 9657-9721, <https://doi.org/10.1021/acs.chemrev.8b00605>.
27. Czarnik, A.W. Chemical Communication in Water Using Fluorescent Chemosensors. *Acc. Chem. Res.* **1994**, *27*, 302-308, <https://doi.org/10.1021/ar00046a003>.
28. Yuan, L.; Lin, W.; Zheng, K.; He, L.; Huang, W. Far-red to near infrared analyte-responsive fluorescent probes based on organic fluorophore platforms for fluorescence imaging. *Chem. Soc. Rev.* **2013**, *42*, 622-661, <https://doi.org/10.1039/C2CS35313J>.
29. Chen, X.; Pradhan, T.; Wang, F.; Kim, J.S.; Yoon, J. Fluorescent Chemosensors Based on Spiroring-Opening of Xanthenes and Related Derivatives. *Chem. Rev.* **2012**, *112*, 1910-1956, <https://doi.org/10.1021/cr200201z>.
30. Wu, H.; Zhang, D.; Su, L.; Ohkubo, K.; Zhang, C.; Yin, S.; Mao, L.; Shuai, Z.; Fukuzumi, S.; Zhu, D. Intramolecular Electron Transfer within the Substituted Tetrathiafulvalene-Quinone Dyads: Facilitated by Metal Ion and Photomodulation in the Presence of Spiropyran. *J. Am. Chem. Soc.* **2007**, *129*, 6839-6846, <https://doi.org/10.1021/ja0702824>.
31. Shibata, H.; Ikeda, Y.; Hiruta, Y.; Citterio, D. Inkjet-printed pH-independent paper-based calcium sensor with fluorescence signal readout relying on a solvatochromic dye. *Anal Bioanal Chem.* **2020**, *412*, 3489-3497, <https://doi.org/10.1007/s00216-019-02218-x>.
32. Jia, L.; Zhang, G.; Zhang, D.; Xiang, J.; Xu, W.; Zhu, D. A new tetrathiafulvalene-phenoxynaphthacenequinone dyad: switching on the intramolecular electron-transfer with UV light irradiation and metal ion coordination. *Chem. Commun.* **2011**, *47*, 322-324, <https://doi.org/10.1039/C0CC02110E>.
33. Boens, N.; Leen, V.; Dehaen, W. Fluorescent indicators based on BODIPY. *Chem. Soc. Rev.* **2012**, *41*, 1130-1172, <https://doi.org/10.1039/C1CS15132K>.
34. Saini, R.; Kaur, N.; Kumar, S. Quinones based molecular receptors for recognition of anions and metal ions. *Tetrahedron* **2014**, *70*, 4285-4307, <https://doi.org/10.1016/j.tet.2014.04.058>.
35. Ghosh, A.; Jose, D.A.; Kaushik, R. Anthraquinones as versatile colorimetric reagent for anions. *Sens. Actuators B Chem.* **2016**, *229*, 545-560, <https://doi.org/10.1016/j.snb.2016.01.140>.
36. Langdon-Jones, E.E.; Pope, S.J.A. The coordination chemistry of substituted anthraquinones: Developments and applications. *Coord. Chem. Rev.* **2014**, *269*, 32-53, <https://doi.org/10.1016/j.ccr.2014.02.003>.
37. Mariappan, K.; Sykes, A.G.J. The chemistry of constrained crown ring systems and fluorescence sensor applications. *Inclusion Phenom. Macrocycl. Chem.* **2013**, *75*, 23-30, <https://doi.org/10.1007/s10847-012-0226-5>.
38. Kalyanasundaram, K.; Thomas, J.K. Solvent-dependent fluorescence of pyrene-3-carboxaldehyde and its applications in the estimation of polarity at micelle-water interfaces. *J. Phys. Chem.* **1977**, *81*, 2176-2180, <https://doi.org/10.1021/j100538a008>.
39. Kadarkaraisamy, M.; Sykes, A.G. Luminescence Detection of Transition and Heavy Metals by Inversion of Excited States: Synthesis, Spectroscopy, and X-ray Crystallography of Ca, Mn, Pb, and Zn Complexes of 1,8-Anthraquinone-18-Crown-5. *Inorg. Chem.* **2006**, *45*, 779-786, <https://doi.org/10.1021/ic051672z>.

40. de Silva, A.P.; Gunaratne, H.Q.N.; Gunnlaugsson, T.; Huxley, A.J.M.; McCoy, C.P.; Rademacher, J.T.; Rice, T.E. Signaling Recognition Events with Fluorescent Sensors and Switches. *Chem. Rev.* **1997**, *97*, 1515-1566, <https://doi.org/10.1021/cr960386p>.
41. Kaur, K.; Kumar, S. 1-Aminoanthracene-9,10-dione based chromogenic molecular sensors: effect of nature and number of nitrogen atoms on metal ion sensing behavior. *Tetrahedron* **2010**, *66*, 6990-7000, <https://doi.org/10.1016/j.tet.2010.06.031>.
42. Kaur, N.; Kumar, S. A differential receptor for selective and quantitative multi-ion analysis for Co²⁺ and Ni²⁺/Cu²⁺. *Tetrahedron Lett.* **2008**, *49*, 5067-5069, <https://doi.org/10.1016/j.tetlet.2008.06.023>.
43. Ranyuk, E.; Uglov, A.; Meyer, M.; Lemeune, A.B.; Denat, F.; Averin, A.; Beletskaya, I.; Guilard, R. Rational design of aminoanthraquinones for colorimetric detection of heavy metal ions in aqueous solution. *Dalton Transactions* **2011**, *40*, 10491-10502, <https://doi.org/10.1039/C1DT10677E>.
44. Kaur, N.; Kumar, S. Single molecular colorimetric probe for simultaneous estimation of Cu²⁺ and Ni²⁺. *Chem. Commun.* **2007**, 3069-3070, <https://doi.org/10.1039/B703529B>.
45. Kaur, N.; Kumar, S. Aminoanthraquinone-based chemosensors: colorimetric molecular logic mimicking molecular trafficking and a set-reset memorized device. *Dalton Trans.* **2012**, *41*, 5217-5224, <https://doi.org/10.1039/C2DT12201D>.
46. Kaur, N.; Kumar, S. A diamide-diamine based Cu²⁺ chromogenic sensor for highly selective visual and spectrophotometric detection. *Tetrahedron Lett.* **2006**, *47*, 4109-4112, <https://doi.org/10.1016/j.tetlet.2006.04.083>.
47. Kaur, N.; Kumar, S. Colorimetric metal ion sensors. *Tetrahedron* **2011**, *67*, 9233-9264, <https://doi.org/10.1016/j.tet.2011.09.003>.
48. Kumar, S.; Kaur, N. Nature of 1-(2-aminoethylamino)-anthracene-9, 10-diones - Cu(II) Interactions Responsible for Striking Colour Changes. *Supramol. Chem.* **2006**, *18*, 137-140, <https://doi.org/10.1080/10610270600564686>.
49. Irving, H.; Williams, R.J.P. 637. The stability of transition-metal complexes. *Journal of the Chemical Society (Resumed)* **1953**, 3192-3210, <https://doi.org/10.1039/JR9530003192>.
50. Kaur, N.; Kumar, S. Colorimetric recognition of Cu(II) by (2-dimethylaminoethyl)amino appended anthracene-9,10-diones in aqueous solutions: deprotonation of aryl amine NH responsible for colour changes. *Dalton Trans.* **2006**, *3*, 3766-3771, <https://doi.org/10.1039/B601558A>.
51. Kaur, N.; Kumar, S. Near-IR region absorbing 1,4-diaminoanthracene-9,10-dione motif based ratiometric chemosensors for Cu²⁺. *Tetrahedron* **2008**, *64*, 3168-3175, <https://doi.org/10.1016/j.tet.2008.01.095>.
52. Ermakova, E.; Michalak, J.; Meyer, M.; Arslanov, V.; Tsvadze, A.; Guilard, R.; Lemeune, A.B. Colorimetric Hg²⁺ Sensing in Water: From Molecules toward Low-Cost Solid Devices. *Org. Lett.* **2013**, *15*, 662-665, <https://doi.org/10.1021/ol303499v>.
53. Ranyuk, E.; Uglov, A.; Meyer, M.; Lemeune, A.B.; Denat, F.; Averin, A.; Beletskaya, I.; Guilard, R. Rational design of aminoanthraquinones for colorimetric detection of heavy metal ions in aqueous solution. *Dalton Trans.* **2011**, *40*, 10491-10502, <https://doi.org/10.1039/C1DT10677E>.
54. Ranyuk, E.; Douaihy, C.M.; Bessmertnykh, A.; Denat, F.; Averin, A.; Beletskaya, I.; Guilard, R. Diaminoanthraquinone-Linked Polyazamacrocycles: Efficient and Simple Colorimetric Sensor for Lead Ion in Aqueous Solution. *Org. Lett.* **2009**, *11*, 987-990, <https://doi.org/10.1021/ol802926m>.
55. Kumar, A.; Vanita, V.; Walia, A.; Kumar, S. N,N-dimethylaminoethylaminoanthrone- A chromofluorogenic chemosensor for estimation of Cu²⁺ in aqueous medium and HeLa cells imaging. *Sens. Actuators, B Chem.* **2013**, *177*, 904-912, <https://doi.org/10.1016/j.snb.2012.11.093>.
56. Wu, S.P.; Du, K.J.; Sung, Y.M. Colorimetric sensing of Cu(II): Cu(II) induced deprotonation of an amide responsible for color changes. *Dalton Trans.* **2010**, *39*, 4363-4368, <https://doi.org/10.1039/B925898A>.
57. Wu, S.P.; Huang, R.Y.; Du, K.J. Colorimetric sensing of Cu(II) by 2-methyl-3-[(pyridin-2-ylmethyl)-amino]-1,4-naphthoquinone: Cu(II) induced deprotonation of NH responsible for color changes. *Dalton Trans.* **2009**, 4735-4740, <https://doi.org/10.1039/B822613J>.
58. Yang, H.; Zhou, Z.-G.; Xu, J.; Li, F.-Y.; Yi, T.; Huang, C.-H. A highly selective ratiometric chemosensor for Hg²⁺ based on the anthraquinone derivative with urea groups. *Tetrahedron* **2007**, *63*, 6732-6736, <https://doi.org/10.1016/j.tet.2007.04.086>.
59. Kim, H.J.; Lee, S.J.; Park, S.Y.; Jung, J.H.; Kim, J.S. Detection of Cu^{II} by a Chemodosimeter-Functionalized Monolayer on Mesoporous Silica. *Adv. Mater.* **2008**, *20*, 3229-3234, <https://doi.org/10.1002/adma.200800246>.
60. Chawla, H.M.; Shukla, R.; Pandey, S. Preferential recognition of zinc ions through a new anthraquinonoidal calix[4]arene. *Tetrahedron Lett.* **2012**, *53*, 2996-2999, <https://doi.org/10.1016/j.tetlet.2012.03.096>.
61. Rasheed, L.; Yousuf, M.; Youn, I.S.; Shi, G.; Kim, K.S. An efficient non-reaction based colorimetric and fluorescent probe for the highly selective discrimination of Pd⁰ and Pd²⁺ in aqueous media. *RSC Adv.* **2016**, *6*, 60546-60549, <https://doi.org/10.1039/C6RA09183K>.
62. Yoshida, K.; Mori, T.; Watanabe, S.; Kawai, H.; Nagamura, T.J. Synthesis and metal ion-sensing properties of fluorescent PET chemosensors based on the 2-phenylimidazo[5,4-a]anthraquinone chromophore. *Chem. Soc., Perkin Trans.* **1999**, *2*, 393-398, <https://doi.org/10.1039/A900424F>.

63. Han, D.Y.; Kim, J.M.; Kim, J.; Jung, H.S.; Lee, Y.H.; Zhang, J.F.; Kim, J.S. ESIPT-based anthraquinonylcalix[4]crown chemosensor for In^{3+} . *Tetrahedron Lett.* **2010**, *51*, 1947-1951, <https://doi.org/10.1016/j.tetlet.2010.02.006>.
64. Okamoto, K.; Fukuzumi, S. An Yttrium Ion-Selective Fluorescence Sensor Based on Metal Ion-Controlled Photoinduced Electron Transfer in Zinc Porphyrin-Quinone Dyad. *J. Am. Chem. Soc.* **2004**, *126*, 13922-13923, <https://doi.org/10.1021/ja045374x>.
65. Agarwal, G.; Lande, D.N.; Chakrovarty, D.; Gejji, S.P.; Mirkute, P.G.; Patil, A.; Gawali, S.S. Bromine substituted aminonaphthoquinones: synthesis, characterization, DFT and metal ion binding studies. *RSC Adv.* **2016**, *6*, 88010-88029, <https://doi.org/10.1039/C6RA20970J>.
66. Parthiban, C.; Manivannan, R.; Elango, K.P. Highly selective colorimetric sensing of Hg(II) ions in aqueous medium and in the solid state via formation of a novel M-C bond. *Dalton Trans.* **2015**, *44*, 3259-3264, <https://doi.org/10.1039/C4DT03289F>.
67. Jali, B.R.; Masud, K.; Baruah, J.B. Selectivity in changes of fluorescence emission of 1,4-naphthoquinone derivatives by manganese and cadmium ions. *Polyhedron* **2013**, *51*, 75-81, <https://doi.org/10.1016/j.poly.2012.12.018>.
68. Mirkute, P.G.; Patil, A.; Lande, D.N.; Chakravarty, D.; Gejji, S.P.; Satpute, S.; Gawali, S.S. Naphthoquinone based chemosensors for transition metal ions: experiment and theory. *RSC Adv.* **2017**, *7*, 55163-55174, <https://doi.org/10.1039/C7RA10490A>.
69. Wang, Y.; Wang, L.; Shi, L.L.; Shang, Z.B.; Zhang, Z.; Jin, W.J. Colorimetric and fluorescence sensing of Cu^{2+} in water using 1,8-dihydroxyanthraquinone- β -cyclodextrin complex with the assistance of ammonia. *Talanta* **2012**, *94*, 172-177, <https://doi.org/10.1016/j.talanta.2012.03.013>.
70. Kar, P.; Suresh, M.; Kumar, D. K.; Jose, D. A.; Ganguly, B.; Das, A. Preferential binding of the magnesium ion by anthraquinone based chromogenic receptors. *Polyhedron* **2007**, *26*, 1317-1322, <https://doi.org/10.1016/j.poly.2006.10.051>.
71. Shamsipur, M.; Poursaberi, T.; Avanes, A.; Sharghi, H. Copper(II)-selective fluorimetric bulk optode membrane based on a 1-hydroxy-9,10-anthraquinone derivative having two propenyl arms as a neutral fluorogenic ionophore. *Spectrochim. Acta, Part A: Mol. Biomol. Spectrosc.* **2006**, *63*, 43-48, <https://doi.org/10.1016/j.saa.2005.04.013>.
72. Park, D.H.; Kang, S.O.; Lee, H.J.; Nam, K.C.; Jeon, S. Synthesis and Electrochemistry of Diester-Anthraquinone as Lithium-Ion Selective Receptor. *Bull. Korean Chem. Soc.* **2001**, *22*, 638-640.
73. Kumar, S.; Pramila, K.; Kaur, S. Photoactive chemosensors. Part 1: A 9,10-anthraquinone and 2-aminothiophenol based Cu(II) selective chemosensor. *Tetrahedron Lett.* **2002**, *43*, 1097-1099, [https://doi.org/10.1016/S0040-4039\(01\)02333-4](https://doi.org/10.1016/S0040-4039(01)02333-4).
74. Mariappan, K.; Basa, P.N.; Balasubramanian, V.; Fuoss, S.; Sykes, A.G. Synthesis, reactivity, catenation and X-ray crystallography of Ag^+ and Cu^+ complexes of anthraquinone-based selenoethers: A luminescent chemodosimeter for Cu^{2+} and Fe^{3+} . *Polyhedron* **2013**, *55*, 144-154, <https://doi.org/10.1016/j.poly.2013.03.003>.
75. Young, V.G.; Quiring, H.L.; Sykes, A.G. A Luminescent Sensor Responsive to Common Oxoacids: X-ray Crystal Structure of $[\text{H}_3\text{O} \cdot 1,8\text{-Oxybis(ethyleneoxyethyleneoxy)anthracene-9,10-dione}]\text{ClO}_4$. *J. Am. Chem. Soc.* **1997**, *119*, 12477-12480, <https://doi.org/10.1021/ol047847a>.
76. Kampmann, B.; Lian, Y.; Klinkel, K.L.; Vecchi, P.A.; Quiring, H.L.; Soh, C.C.; Sykes, A.G. Luminescence and Structural Comparisons of Strong-Acid Sensor Molecules. 2. *J. Org. Chem.* **2002**, *67*, 3878-3883, <https://doi.org/10.1021/jo0257344>.
77. Kadarkaraisamy, M.; Sykes, A.G. Selective luminescence detection of cadmium(II) and mercury(II) utilizing sulfur-containing anthraquinone macrocycles (part 2) and formation of an unusual -crown ether dimer via reduction of Hg(II) by DMF. *Polyhedron* **2007**, *26*, 1323-1330, <https://doi.org/10.1016/j.poly.2006.10.046>.
78. Basa, P.N.; Bhowmick, A.; Schulz, M.M.; Sykes, A.G. Site-Selective Imination of an Anthracenone Sensor: Selective Fluorescence Detection of Barium(II). *J. Org. Chem.* **2011**, *76*, 7866-7871, <https://doi.org/10.1021/jo2013143>.
79. Kim, H.J.; Kim, S.H.; Kim, J.H.; Anh, L.N.; Lee, J.H.; Lee, C.H.; Kim, J.S. ICT-based Cu(II)-sensing 9,10-anthraquinonecalix[4]crown. *Tetrahedron Lett.* **2009**, *50*, 2782-2786, <https://doi.org/10.1016/j.tetlet.2009.03.149>.
80. Kim, S.H.; Choi, H.S.; Kim, J.; Lee, S.J.; Quang, D.T.; Kim, J.S. Novel Optical/Electrochemical Selective 1,2,3-Triazole Ring-Appended Chemosensor for the Al^{3+} Ion. *Org. Lett.* **2010**, *12*, 560-563, <https://doi.org/10.1021/ol902743s>.
81. Zhang, Y.J.; He, X.P.; Hua, M.; Li, Z.; Shi, X.X.; Chen, G.R. Highly optically selective and electrochemically active chemosensor for copper (II) based on triazole-linked glucosyl anthraquinone. *Dyes Pigments*, **2011**, *88*, 391-395, <https://doi.org/10.1016/j.dyepig.2010.08.010>.
82. Erk, C.; Erbay, E. Novel Macrocycles. Part 6. Synthesis, Structures and Cation Binding from Optical Spectroscopy of 9,10-Anthraquinone-crown Ethers. *J. Inclusion Phenom. Macrocycl. Chem.* **2000**, *36*, 229-241, <https://doi.org/10.1023/A:1008072926866>.
83. Ghosh, K.; Kar, D. Anthraquinone coupled benzothiazole-based receptor for selective sensing of Cu^{2+} . *J. Inclusion Phenom. Macrocycl. Chem.* **2013**, *77*, 67-74, <https://doi.org/10.1007/s10847-012-0217-6>.

84. Kursunlu, A.N. A fluorescent “turn on” chemosensor based on Bodipy-anthraquinone for Al(III) ions: synthesis and complexation/spectroscopic studies. *RSC Adv.*, **2015**, *5*, 41025-41032, <https://doi.org/10.1039/C5RA03342J>.
85. Zhan, J.; Fang, F.; Tian, D.; Li, H. Anthraquinone-modified calix[4]arene: Click synthesis, selective calcium ion fluorescent chemosensor and INHIBIT logic gate. *Supramol. Chem.* **2012**, *24*, 272–278, <https://doi.org/10.1080/10610278.2012.656124>. (b) Lv, X.-X.; Wang, Q.; Zhang, L.-J.; Lu, L.-L.; Zhao, M.; Guo, D.-S. Synthesis, crystal structure and remote allosteric binding properties of cone thiacalix[4]pseudocrown receptors bearing anthraquinone function and different arms. *RSC Adv.* **2017**, *7*, 35528-35536, <https://doi.org/10.1039/C7RA06083A>.
86. Bhalla, V.; Gupta, A.; Kumar, M. A pentacenequinone derivative with aggregation-induced emission enhancement characteristics for the picogram detection of Fe³⁺ ions in mixed aqueous media. *Dalton Trans.* **2013**, *42*, 4464-4469, <https://doi.org/10.1039/C3DT32546F>.
87. Bhalla, V.; Gupta, A.; Kumar, M. Fluorescent Nanoaggregates of Pentacenequinone Derivative for Selective Sensing of Picric acid in Aqueous Media. *Org. Lett.* **2012**, *14*, 3112-3115, <https://doi.org/10.1021/ol301202v>.
88. Bhalla, V.; Gupta, A.; Kumar, M. Nanoaggregates of a pentacenequinone derivative as reactors for the preparation of palladium nanoparticles. *Chem. Commun.* **2012**, *48*, 11862-11864, <https://doi.org/10.1039/C2CC36667C>.
89. Bhalla, V.; Roopa; Kumar, M.; Sharma, P.R.; Kaur, T. Hg²⁺ induced hydrolysis of pentaquinone based Schiff base: a new chemodosimeter for Hg²⁺ ions in mixed aqueous media. *Dalton Trans.* **2013**, *42*, 15063-15068, <https://doi.org/10.1039/C3DT51273H>.
90. Bhalla, V.; Roopa; Kumar, M. Pentaquinone based probe for nanomolar detection of zinc ions: Chemosensing ensemble as an antioxidant. *Dalton Trans.* **2013**, *42*, 975-980, <https://doi.org/10.1039/C2DT31341C>.
91. Bhalla, V.; Kumar, M. Fluoride Triggered Fluorescence “Turn On” Sensor for Zn²⁺ Ions Based on Pentaquinone Scaffold That Works as a Molecular Keypad Lock. *Org. Lett.* **2012**, *14*, 2802-2805, <https://doi.org/10.1021/ol301030z>.
92. Liu, R.L.; Lu, H.Y.; Li, M.; Z.Hu S.; Chen, C.F. Simple, efficient and selective colorimetric sensors for naked eye detection of Hg²⁺, Cu²⁺ and Fe³⁺. *RSC Adv.* **2012**, *2*, 4415-4420, <https://doi.org/10.1039/C2RA20385E>.
93. Zeng, Y.; Zhang, G.; Zhang, D.; Zhu, D. A dual-function colorimetric chemosensor for thiols and transition metal ions based on ICT mechanism. *Tetrahedron Lett.* **2008**, *49*, 7391-7394, <https://doi.org/10.1016/j.tetlet.2008.10.055>.
94. Jali, B.R.; Baruah, J.B. Fluorescence properties, aluminium ion selective emission changes and self-assemblies of positional isomers of 4-(hydroxyphenylthio) naphthalene-1,2-diones. *Dyes Pigments* **2014**, *110*, 56-66, <https://doi.org/10.1016/j.dyepig.2014.05.023>.
95. Vogtle, F. New ligand systems for ions and molecules and electronic effects upon complexation. *Pure Appl. Chem.* **1980**, *52*, 2405-2416, <http://dx.doi.org/10.1351/pac198052112405>.
96. Kim, J.Y.; Kim, G.; Kim, C.R.; Lee, S.H.; Lee, J.H.; Kim, J.S. UV band splitting of chromogenic azo-coupled calix[4]crown upon cation complexation. *J. Org. Chem.* **2003**, *68*, 1933-1937, <https://doi.org/10.1021/jo020684o>.
97. Wu, H.; Zhang, D.; Su, L.; Ohkubo, K.; Zhang, C.; Yin, S.; Mao, L.; Shuai, Z.; Fukuzumi, S.; Zhu, D. Intramolecular Electron Transfer within the Substituted Tetrathiafulvalene-Quinone Dyads: Facilitated by Metal Ion and Photomodulation in the Presence of Spiropyran. *J. Am. Chem. Soc.* **2007**, *129*, 6839-6846, <https://doi.org/10.1021/ja0702824>.
98. Jia, L.; Zhang, G.; Zhang, D.; Xiang, J.; Xu, W.; Zhu, D. A new tetrathiafulvalene-phenoxynaphthacenequinone dyad: switching on the intramolecular electron-transfer with UV light irradiation and metal ion coordination. *Chem. Commun.* **2011**, *47*, 322-324, <https://doi.org/10.1039/C0CC02110E>.